JCB Article

Myosin 1c and myosin IIB serve opposing roles in lamellipodial dynamics of the neuronal growth cone

Thomas J. Diefenbach, Vaughan M. Latham, Dean Yimlamai, Canwen A. Liu, Ira M. Herman, and Daniel G. Jay

Department of Physiology, Tufts University School of Medicine, Boston, MA 02111

The myosin family of motor proteins is implicated in mediating actin-based growth cone motility, but the roles of many myosins remain unclear. We previously implicated myosin 1c (M1c; formerly myosin Iβ) in the retention of lamellipodia (Wang et al., 1996). Here we address the role of myosin II (MII) in chick dorsal root ganglion neuronal growth cone motility and the contribution of M1c and MII to retrograde F-actin flow using chromophore-assisted laser inactivation (CALI). CALI of MII reduced neurite outgrowth and growth cone area by 25%, suggesting a role for MII in lamellipodial expansion. Micro-CALI of MII caused a rapid reduction in local lamellipodial protrusion in growth cones with no effects on filopodial dynamics. This is opposite to micro-CALI of M1c, which caused an increase in lamellipodial protrusion. We used fiduciary beads (Forscher et al., 1992) to observe retrograde F-actin flow during the acute loss of M1c or MII. Micro-CALI of M1c reduced retrograde bead flow by 76%, whereas micro-CALI of MII or the MIIB isoform did not. Thus, M1c and MIIB serve opposite and nonredundant roles in regulating lamellipodial dynamics, and M1c activity is specifically required for retrograde F-actin flow.

Introduction

During development of the nervous system, the neuronal growth cone advances in response to diverse cues during axon guidance. The molecular mechanisms underlying growth cone motility remain unclear. One suggested mechanism is the clutch hypothesis (Mitchison and Kirschner, 1988), which is also used to explain the mechanics underlying some aspects of actin-based cell migration (Svitkina et al., 1997). The clutch hypothesis states that forward movement of the growth cone is coupled to retrograde flow, the rearward movement of F-actin by treadmilling in concert with the action of molecular motors (Forscher and Smith, 1988; Mitchison and Kirschner, 1988; Suter and Forscher, 2000). This notion has been supported by showing that growth cone advance is inversely proportional to retrograde flow in *Aplysia* growth cones in culture (Lin and Forscher, 1995). BDM (2,3-butanedione monoxime), a general inhibitor of most myosin ATPases (although not nonmuscle myosin II [MII]*) (Cheung et al., 2002), decreases retrograde flow and causes concomitant growth at the leading edge of *Aplysia* neurons in culture (Lin et al., 1996). These findings suggest that myosin(s) are required for growth cone motility. However, the identity of the myosin isoforms required and how they function in leading edge motility remains unclear.

There are at least 18 members of the myosin superfamily (Berg et al., 2001), four of which have been observed in neuronal growth cones (myosin I [MI], MII, myosin V [MV], and myosin VI) (Ruppert et al., 1993; Rochlin et al., 1995; Suter et al., 2000). MV and myosin Iβ have been tested directly for specific functions in the growth cone (Wang et al., 1996). Myosin 1c (M1c; formerly myosin Iβ) (Gillespie et al., 2001) is a single headed myosin (for review see Coluccio, 1997) expressed in the peripheral domain of growth cones (Wagner et al., 1992) whose short tail binds membranes and actin (Bahler et al., 1994). Micro–chromophore-assisted laser inactivation (CALI) of M1c in growth cones of chick dorsal root ganglion (DRG) caused local lamellipodial extension into the laser light, suggesting that it is involved in the retention of lamellipodia (Wang et al., 1996), but it is unclear how M1c functions in this process. MII, the conventional, two-headed, nonmuscle myosin, is found at the leading edge of rapidly migrating cells (Svitkina et al., 1997) and in the peripheral region of growth cones in proximity with the plasma membrane (Cheng et al., 1992; Miller et al., 1992). Previous studies have implicated MII function in neurite

Address correspondence to Daniel G. Jay, Dept. of Physiology, Tufts University School of Medicine, 136 Harrison Ave., Boston, MA, 02111. Tel.: (617) 636-2957. Fax: (617) 636-0445. E-mail: djay01@emerald.tufts.edu

T.J. Diefenbach and V.M. Latham contributed equally to this work.

M. Latham's present address is Dept of Adult Oncology, Dana Farber Cancer Institute, 44 Binney St., Boston MA 02115.

*Abbreviations used in this paper: CALI, chromophore-assisted laser inactivation; DRG, dorsal root ganglion; MG, malachite green isothiocyanate; M1c, myosin 1c; MI, myosin I; MII, myosin II; MSD, mean squared displacement; MV, myosin V.

Key words: CALI; growth cones; lamellipodia; Myo1c; myosin Iβ

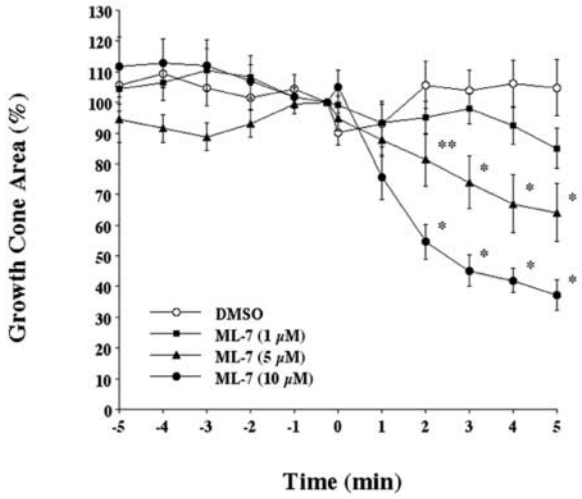

Figure 1. **Pharmacological inhibition using ML-7 leads to a reduction in growth cone area.** ML-7 was applied to cultures for a 5-min period followed by rapid washout. There was a significant dose-dependent reduction in growth cone area with increasing concentrations of ML-7 (*$P < 0.01$; **$P < 0.05$). Number of growth cones: DMSO, 10; ML-7 (1.0 μM), 9; ML-7 (5.0 μM), 10; ML-7 (10 μM), 11.

outgrowth (Ruchhoeft and Harris, 1997; Wylie et al., 1998; Tullio et al., 2001; Wylie and Chantler, 2001) and growth cone morphology (Bridgman et al., 2001), but the precise cellular role was not established. Here, we address directly the roles of M1c and MII on growth cone motility and retrograde F-actin flow using CALI (Jay, 1988; Buchstaller and Jay, 2000).

Results

We directly addressed the role of MII in DRG neurons by three approaches: pharmacological inhibition (Ruchhoeft and Harris, 1997), large scale CALI (Jay, 1988), and micro-CALI during time-lapse video microscopy (Wang et al., 1996). The application of micro-CALI allows us to track dynamic changes in growth cone morphology and neurite outgrowth rates during the acute loss of MII without compensation that may be associated with chronic loss of function.

We used the specific MII inhibitor, ML-7 (Saitoh et al., 1987) to inhibit MII function in chick DRG growth cones. ML-7 was used previously to study MII function in *Xenopus* retinal axon outgrowth and caused decreased axonal outgrowth and collapsed growth cones (Ruchhoeft and Harris, 1997). Due to the diversity of myosin isoform expression and differential efficacy of myosin inhibitors for different cell types, it is necessary to show that ML-7 is effective in chick DRG neurons in culture. Chick DRG growth cone area decreased markedly in response to acute addition of ML-7 in a dose-dependent fashion (1–10 μM) (Fig. 1). We observed a significant percentage of growth cones that underwent collapse and neurite retraction with 5.0 μM ML-7 (40% of growth cones collapsed; $P < 0.005$, $n = 10$) and an even greater incidence of collapse with 10 μM ML-7, (100%; $P < 0.0001$, $n = 11$). With 1.0 μM ML-7, none of the growth cones collapsed ($n = 9$). These findings agree with previous studies (Ruchhoeft and Harris, 1997) and suggest a role for

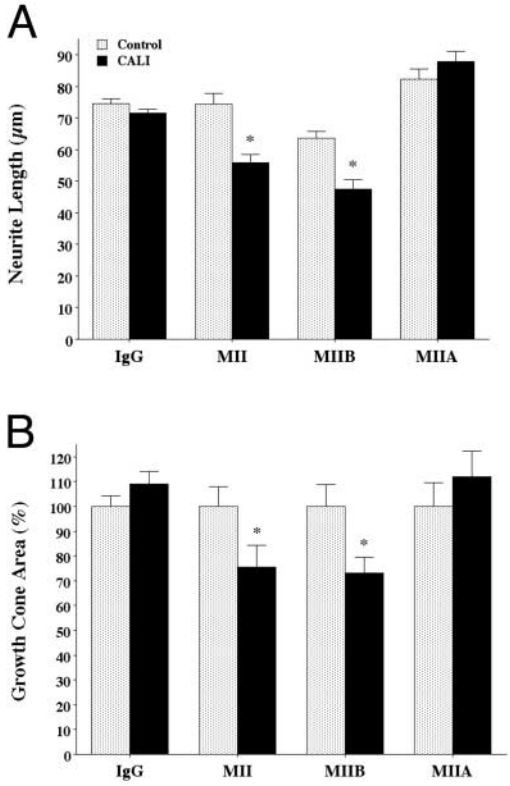

Figure 2. **Whole-cell CALI using the MII antibody results in reduced neurite outgrowth and growth cone area comparable to the effects of pharmacological inhibition.** (A) Control, unirradiated neurons (gray bars); neurons which received CALI treatment (black bars). There was a 26% reduction in neurite length with CALI of MII compared with unirradiated neurons (*$P < 0.001$; number of growth cones: MII Control, 77; MII CALI, 118). CALI of neurons loaded with MIIB antibody showed a similar 25% reduction in neurite length over the same 1-h period (*$P < 0.001$; MIIB Control, 98; MIIB CALI, 79). In contrast, neurons loaded with MIIA antibody (MIIA Control, 264; MIIA CALI, 217) or nonspecific MG-IgG (IgG Control, 286; IgG CALI, 270) showed no change in neurite length over the same period compared with unirradiated neurons. (B) Whole-cell CALI of MII results in reduced growth cone area. Growth cones loaded with MII antibody and irradiated for 2 min had areas 25% less than unirradiated growth cones 1 h after treatment (*$P < 0.05$; MII Control, 72; MII CALI, 86). CALI of MIIB-loaded neurons had an effect similar to that of MII (MIIB control, 82; MIIB CALI, 43). CALI of MIIA (MIIA Control, 28; MIIA CALI, 31) and of MG-IgG controls (MG-IgG Control, 209; MG-IgG CALI, 173) yielded no changes in growth cone area.

MII in DRG growth cone morphology. We next compared CALI of MII with pharmacological inhibition.

We performed large scale CALI of MII on populations of cultured DRG neurons. CALI of MII resulted in a specific and significant reduction in neurite length over the 1-h post-treatment period (26%, $P < 0.0001$) compared with malachite green isothiocyanate (MG)–anti-MII–loaded neurites on the unirradiated side of the dish (Fig. 2 A). CALI was performed using nonspecific MG-IgG on neurons from the same chick embryos at the same time. These neurons showed no change in neurite length over the 1-h period. These results support a role for MII in neurite outgrowth. CALI of MII shows a comparable decrease in outgrowth to that seen after ML-7 application or antisense perturbation of

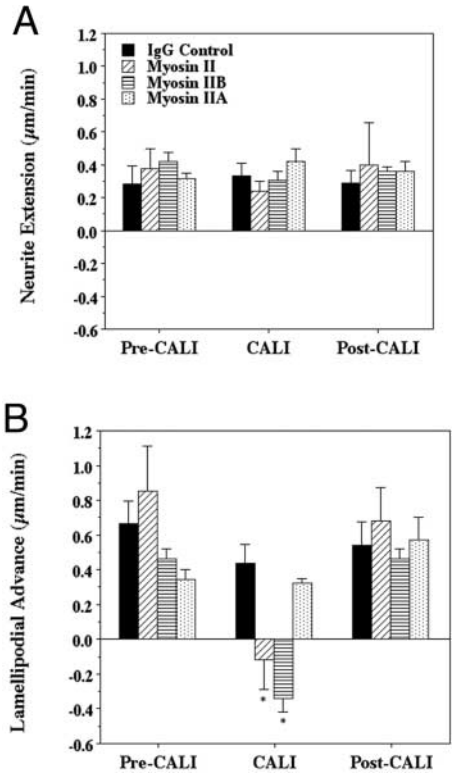

Figure 3. **Micro-CALI of entire growth cones leads to retraction of the leading edge without altering the rate of neurite outgrowth.** (A) The rate of advance of the neurite neck (a measure of neurite outgrowth) and the leading edge (B; a measure of the forward extension of the growth cone) were determined for three 5-min intervals: before micro-CALI (Pre-CALI), during micro-CALI (CALI), and after micro-CALI (Post-CALI). The effect of MII inactivation was first apparent by 1 min after onset of irradiation and persisted for the duration of treatment. This effect on the leading edge was transient, since there was recovery to the preCALI level of extension within the first 5 min after micro-CALI. Number of growth cones: IgG, 14; MII, 12; MIIB, 10; MIIA, 10. *$P < 0.005$.

MII (Wylie et al., 1998; Wylie and Chantler, 2001). These findings with CALI are consistent with those using pharmacological or antisense RNA approaches. Growth cone area was also reduced in response to CALI of MII (25%, $P < 0.05$) (Fig. 2 B), whereas CALI using a nonspecific IgG had no effect. Loading of MG–anti-MII had no effect on neurite length or growth cone area, showing that anti-MII is not function blocking without laser irradiation. These findings suggest a role for MII in regulating growth cone morphology. Therefore, we examined the effects of local and rapid loss of MII function using micro-CALI.

Micro-CALI of MII was performed over the whole growth cone area for 5 min, and changes in outgrowth rate and growth cone morphology were monitored using time-lapse video microscopy. There was no significant change in the rate of forward advance of the neurite neck as a result of micro-CALI of MII (Fig. 3 A) ($n = 13$). Thus, the presumed loss of MII function acutely in the growth cone did not alter the instantaneous rate of neurite extension. Instead, micro-CALI of MII leads to a significant retraction of leading edge lamellipodia (Fig. 3 B) ($P < 0.005$, $n = 13$). Lamellipodial retraction was also assessed by measuring

Table I. **Rates of filopodial extension and retraction are unaffected by micro-CALI of MII**

	Control side	Side receiving micro-CALI
	μm/min	
Filopodial extension		
IgG control	0.068 ± 0.007	0.070 ± 0.007
MII	0.062 ± 0.006	0.052 ± 0.005
Filopodial retraction		
IgG control	0.073 ± 0.009	0.068 ± 0.005
MII	0.071 ± 0.004	0.067 ± 0.006

Rates of filopodial extension and retraction were determined for irradiated and unirradiated growth cone sides by averaging the rate of extension and retraction over the 5-min period. Length measurements were obtained at 30-s intervals and expressed as μm/min. There were no significant differences in the rate of extension or retraction on the control versus irradiated sides of growth cones. Number of filopodia: MII, 87; IgG, 57.

growth cone area before, during, and after micro-CALI of MII (Figs. 4 and 5). Prior to micro-CALI, there were no significant differences in the rates of neurite extension or leading edge movement in the different treatment groups (Student's *t* test). Growth cones loaded with MII antibody and irradiated for 5 min over their entire area displayed a rapid 24 ± 3.4% reduction in total area (Fig. 5 C) ($P < 0.0001$, $n = 13$). Interestingly, when MII was inactivated over half a growth cone, the reduction in growth cone area (Fig. 4 B and Fig. 5 B) (39 ± 4.3%, $n = 21$) was significantly greater than that seen when MII was uniformly inactivated across the entire growth cone ($P < 0.05$). This may be due to the imbalance of tension resulting from asymmetric loss of MII compared with the uniform loss of MII over the entire growth cone. Growth cones loaded with MG-IgG showed no change in area both during and after local irradiation (Fig. 4 A and Fig. 5 A). These findings suggest that MII plays a role in lamellipodial extension.

In contrast to the effect of micro-CALI of MII on lamellipodia, there were no concomitant changes in filopodial dynamics during this treatment. MII inactivation produced no changes in the summed lengths of filopodia measured at 1-min intervals over the 5-min treatment period (unpublished data). Both the rates of filopodial extension and retraction were quantified as done previously for MV (Wang et al., 1996). Inactivation of MII yielded no significant effects on the rate of filopodial extension or retraction (Table I). We also divided the population of filopodia into 5 μm size classes (1–5 μm, 5–10 μm, 10–15 μm, etc.) to determine if inactivation of MII selectively affected the number of longer or shorter filopodia. This analysis yielded no significant changes in several of the filopodial size classes (unpublished data) with the exception of the 1–5 μm size class. These smallest filopodia showed a 30% reduction in number by the end of the 5-min treatment period ($P < 0.05$, $n = 43$). This size class may be more susceptible to retraction of lamellipodia because their actin bundles do not extend into the growth cone transition zone where they can interact with microtubules (Dent and Kalil, 2001). Together, these results show that MII activity is not essential for filopodial dynamics.

These findings suggest that MII plays a role in lamellipodial extension. This is opposite to the role of M1c. Previ-

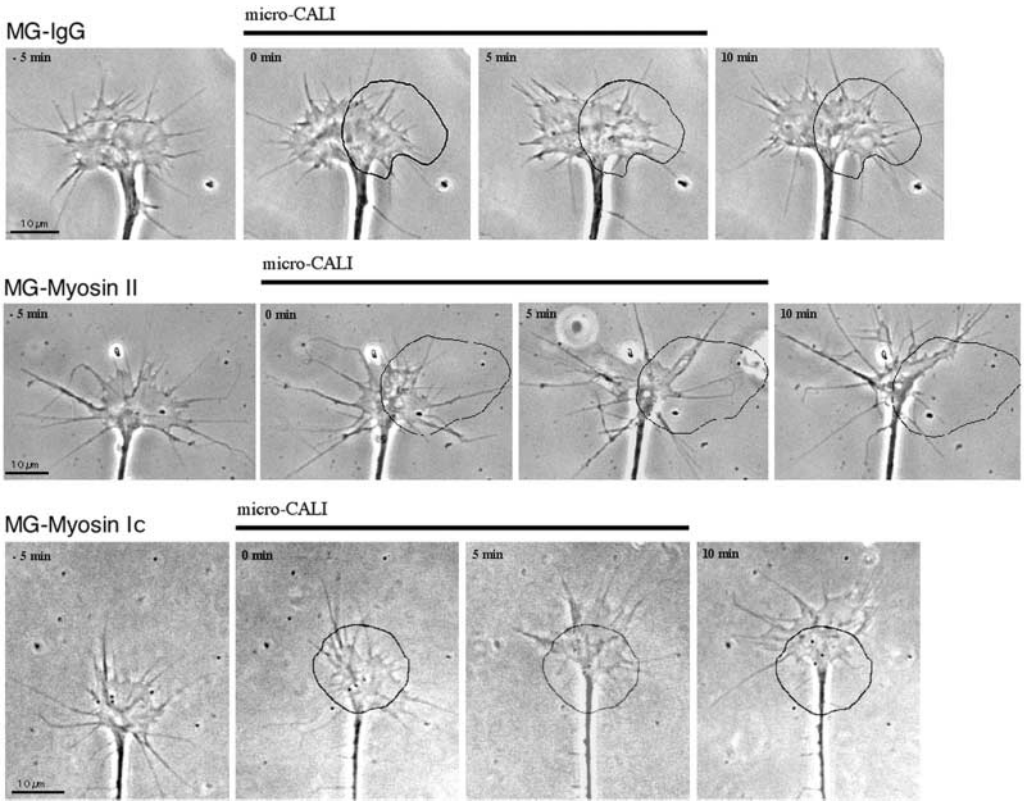

Figure 4. **Micro-CALI of MII and M1c have opposing effects on growth cone motility.** (A) Growth cones loaded with MG-IgG antibody were irradiated for 5 min on one half with the other half serving as an internal control. Images were captured 5 min before micro-CALI (−5 min), at the beginning of micro-CALI (0 min), at the end of a 5-min micro-CALI treatment (5 min), and 10 min after treatment (10 min). The irregular line delineates the perimeter of the laser spot. Asymmetric inactivation of nonspecific MG-IgG had no effect on growth cone motility or shape. (B) Asymmetric inactivation of MII resulted in retraction of lamellipodia within the 5-min treatment period, an effect that in some instances continued after irradiation ceased. (C) In contrast to the effect of MII inactivation, micro-CALI of M1c over the entire growth cone resulted in lamellipodial expansion into the laser spot. Although this particular growth cone showed an increase in neurite extension during micro-CALI, this was not consistently observed.

ously, we showed that inactivation of M1c over part of the growth cone resulted in lamellipodial protrusion (Wang et al., 1996) and suggested that M1c had a role in lamellipodial retention (limiting protrusion). Here we tested the effect of inactivation of M1c over the entire growth cone and found an increase in growth cone area (15 ± 2.3%, $n = 8$) (Fig. 4 C) that was significantly different than unirradiated controls ($P < 0.001$), although not as large as we had seen with asymmetric micro-CALI of M1c over part of the growth cone.

We analyzed the local movements of individual lamellipodia to address the cellular role of M1c or MII in lamellipodial behavior. We measured lamellipodial dynamics on the front half of the growth cone, since the front contributes to forward advance of the growth cone, whereas the rear consolidates into the nascent neurite. Also, the rear of the growth cone proximal to the neurite shaft was often devoid of lamellar veils. We quantified net lamellipodial displacement by taking a point on the leading edge halfway between two filopodia and measuring the distance it covered during the 5-min micro-CALI treatment. In control growth cones, there was no difference in the amount of lamellipodial protrusion and retraction. Micro-CALI of M1c caused a significantly greater local protrusion compared with MG-IgG–loaded control ($P < 0.05$) (Table II) without affecting retraction. Conversely, micro-CALI of MII significantly reduced local lamellipodial protrusion compared with control ($P < 0.05$) (Tables II and III), again without affecting lamellipodial retraction.

Table II. **Opposing effects of micro-CALI of M1c and MII in lamellipodial protrusion**

Net displacement	Protrusion	Retraction
	μm	
IgG control	2.6 ± 0.3 (42)	2.0 ± 0.3 (19)
M1c	3.5 ± 0.3 (54)[a]	1.9 ± 0.4 (27)
MII	1.7 ± 0.2 (33)[a]	2.0 ± 0.2 (31)

[a]Significant difference in protrusion relative to IgG control ($P < 0.05$).
The distance in μm covered by the center of each lamellipodium (at the midpoint between adjacent filopodia) was determined for the 5-min micro-CALI treatment period. The distances were averaged for all the lamellipodia in the front half of the growth cone (Net displacement). Numbers in parentheses indicate the number of lamellipodia.

Since the effect of M1c and MII on net lamellipodial protrusion could be the result of an increase in the number of lamellipodia that protrude, we also examined the proportion of protruding, retracting, and stationary lamellipodia (Table III). Micro-CALI of M1c did not alter this proportion compared with IgG controls, whereas micro-CALI of MII significantly decreased the proportion of protruding lamellipodia (46%; $n = 9$, $P < 0.05$) and increased the

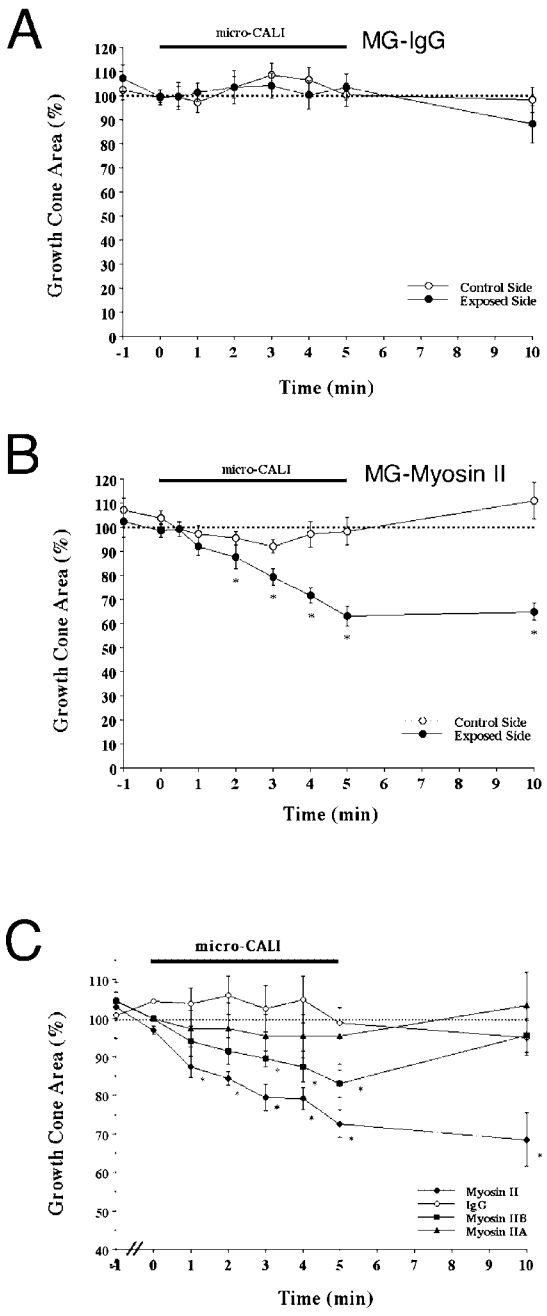

Figure 5. **The effect of MII inactivation is quantifiable and specific to the MIIB isoform.** (A) Local irradiation of MG-IgG–loaded growth cones on one side causes no change in area on either exposed or unexposed sides ($n = 13$). (B) In contrast, inactivation of MII reduces growth cone area specifically on the exposed side, with no consistent change in area on the unexposed side. Growth cones loaded with MII antibody and exposed for 5 min on one side showed a significant 39 ± 4.3% reduction in growth cone area on the irradiated side relative to the control, unirradiated side (*$P < 0.001$, $n = 21$). (C) Micro-CALI of entire growth cones yields similar results as seen in half-growth cone exposures. Growth cones loaded with MII displayed a significant reduction in total area within 1 min after onset of treatment, leading to a 24 ± 3.4% reduction by the end of the 5-min treatment period (*$P < 0.0001$, $n = 13$). Micro-CALI of MIIB similarly reduced growth cone area by 3 min after onset ofirradiation, leading to a 17% reduction by the end of the treatment period (17%; $P < 0.01$, $n = 20$). In contrast, micro-CALI of MIIA ($n = 9$) and MG-IgG ($n = 10$) had no effect.

proportion of stationary lamellipodia (13%; $n = 9$, $P < 0.05$). The analysis of lamellipodial dynamics showed that micro-CALI of M1c increased net protrusion without affecting the proportion of protruding lamellipodia, whereas micro-CALI of MII reduced net protrusion and reduced the proportion of protruding lamellipodia. These findings show that M1c and MII function by altering lamellipodial protrusion at the leading edge without affecting lamellipodial retraction.

Our results suggest that M1c acts in the clutch mechanism (its localized loss increases lamellipodial protrusion), although it was postulated previously that MII serves this role (Hasson and Mooseker, 1997; Svitkina et al., 1997). We tested which myosin couples lamellipodial movement to retrograde F-actin flow by observing the movement of flow-coupled 200 nm microbeads (Lin and Forscher, 1995) during micro-CALI of MII or M1c. First, we validated the assay by comparing the bead flow rate with the flow of rhodamine-labeled actin in filopodia of chick DRG neurons. The average rate of retrograde bead flow was 4.3 ± 1.6 μm/min ($n = 6$), similar to the retrograde movement of microinjected rhodamine-labeled actin (4.6 ± 1.0 μm/min, $n = 12$) and similar to the rate reported for bead movement on *Aplysia* growth cones (4.46 ± 2.13 μm/min) (Lin and Forscher, 1995).

To address the roles of M1c and MII in retrograde flow in lamellipodia, we bath-applied microbeads to neurons loaded with either MG–anti-M1c, MG–anti-MII, or MG-IgG. Microbeads on growth cone lamellipodia were imaged at 3-s intervals, and their movement was tracked before, during, and after micro-CALI. Beads displayed centripetal movement (movement from the leading edge of a lamellipodium toward the central region) (Fig. 6, B and C). We observed an average rate of retrograde bead movement on lamellipodia of 1.56 ± 0.24 μm/min ($n = 22$), a rate comparable to that reported previously for lamellipodia (Welnhofer et al., 1999) but less than flow rates on filopodia (Forscher and Smith, 1988; Lin and Forscher, 1995; Danuser and Oldenbourg, 2000). In some instances, centripetal movement was interrupted by lateral diffusive movements, followed by movement along a new centripetal path (Fig. 6 C).

Micro-CALI of M1c caused a 76% reduction in retrograde flow compared with unirradiated, control growth cones ($P < 0.05$) (Fig. 6 D). Thus, we observed lamellipodial expansion across the entire growth cone concomitant with a decrease in retrograde flow upon the loss of M1c activity. Since it has been reported that there is an inverse relationship between retrograde bead flow and filopodial extension (Lin and Forscher, 1995), we compared the rate of bead flow to the rate of protrusion of lamellipodia immediately adjacent to beads in M1c growth cones and found no correlation (linear regression, $r^2 = 0.582$, $n = 7$). In contrast to the effect of micro-CALI of M1c, micro-CALI of MII and all control treatments had no significant effect on retrograde flow. Instead, micro-CALI of MII caused a 95% decrease in lateral bead diffusion (significantly different than the unirradiated control; $P < 0.001$) (Fig. 6 E), whereas micro-CALI of M1c had no observable effect on lateral bead diffusion rates. Together, these findings indicate that M1c and not MII is required for retrograde flow and links M1c-mediated

Table III. **Distinct effects of micro-CALI of M1c and MII on the proportion of protruding lamellipodia**

Lamellipodial behavior	Protrusion	Retraction	Stationary
		%	
IgG control	74.9 ± 7.7 (9)	20.8 ± 6.7 (9)	4.2 ± 2.1 (9)
M1c	60.4 ± 8.8 (10)	31.3 ± 7.9 (10)	6.7 ± 2.7 (10)
MII	46.4 ± 10.7 (9)[a]	39.6 ± 9.8 (9)	12.5 ± 2.8 (9)[a]

[a]Significant difference relative to IgG control ($P < 0.05$).
For lamellipodial behavior, the proportions of protruding, retracting, and stationary lamellipodia were determined and expressed as the percentage of the total number of lamellipodia for that group. Numbers in parentheses indicate the number of growth cones.

retrograde flow with lamellipodial extension as suggested by the clutch hypothesis.

Given the effect of MII on lamellipodia, we investigated whether one of the MII isoforms expressed in neurons and their growth cones is responsible for the effects observed with the general MII antibody. Recent studies have suggested that two MII isoforms, MIIA and MIIB, have different roles in neurite outgrowth and cell adhesion (Wylie and Chantler, 2001). We confirm the following findings: CALI or micro-CALI of MIIB showed similar results to MII in neurite outgrowth (Fig. 2 A and Fig. 3 A), growth cone morphology (Fig. 2 B, Fig. 3 B, and Fig. 5 C), and in retrograde flow and bead diffusion (Fig. 6, D and E), whereas micro-CALI of MIIA had no significant effects on any of the morphological parameters (Fig. 2, A and B, Fig. 3, A and B, and Fig. 5 C). These findings support a role for the MIIB isoform in lamellipodial protrusion.

Discussion

Here we present evidence that M1c and MIIB play opposing roles in lamellipodial motility of the neuronal growth cone. We have shown that M1c and MIIB inactivation results in growth cone expansion and retraction, respectively. Pharmacological inhibition, CALI, and micro-CALI of MII or MIIB all resulted in lamellipodial retraction. Inactivation of MII or MIIB had no effect on retrograde flow rates and caused lamellipodial retraction, a result opposite to what would be expected if MII powered retrograde flow (Lin and Forscher, 1995). In contrast, micro-CALI of M1c caused lamellipodial expansion and a significant decrease in retrograde flow. Analyses of lamellipodial dynamics during micro-CALI showed that M1c and MII both act during protrusion but in opposing directions. Our findings illustrate that expansion and retraction of lamellipodia are regulated by distinct processes as has been previously demonstrated for filopodial extension

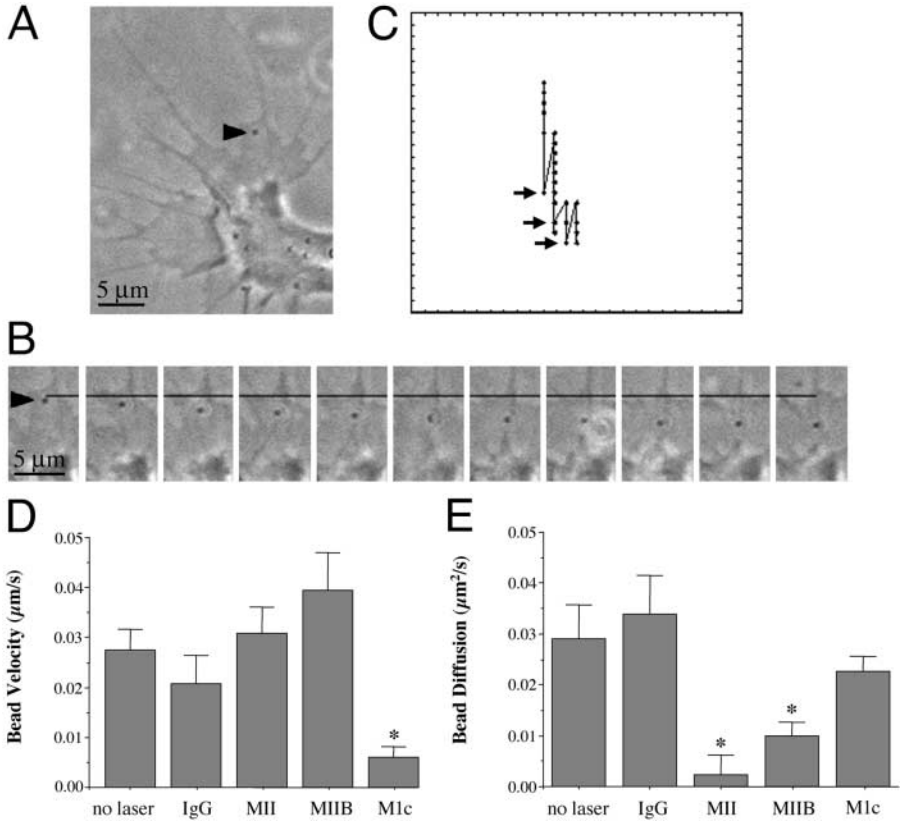

Figure 6. **M1c and MII differentially affect retrograde F-actin flow.** (A) A phase–contrast micrograph of a growth cone with a single bead on the lamellipodium (arrowhead). (B) Image series shown at 12-s intervals of the same bead in A proceeding retrogradely toward the central region (bottom of panel), demonstrating that 200 nm beads show retrograde flow on chick DRG growth cones. The line provides a reference point for the starting position of the bead. (C) Bead movements sampled at 3-s intervals could be plotted as x,y coordinates on a two-dimensional plane. A plot of the directed and diffusive movements of the same bead over the time period represented in B is shown with arbitrary scales. The top-most point is closest to the leading growth cone edge and corresponds to the bead shown in A or the first panel in B. The black arrows indicate points preceding lateral transitions in motion. (D) Growth cones loaded with either MII or MIIB showed no differences in the velocity of bead movement compared with matched MG-IgG–loaded controls, whereas growth cones loaded with M1c displayed a significant 76% reduction in velocity (*$P < 0.05$). (E) Micro-CALI of MII and MIIB had a significant effect on the diffusion rate of beads, with MII-loaded growth cones showing a 95% reduction in random bead diffusion (*$P < 0.001$) and MIIB-loaded growth cones showing an 80% reduction in diffusion (*$P < 0.05$), whereas M1c inactivation was without effect on bead diffusion. Number of beads for D and E: no laser, 22; IgG (with laser), 16; MII, 18; MIIB, 12; M1c, 14.

and retraction (Wang et al., 1996; Lu et al., 1997). Our findings directly implicate M1c in lamellipodial retrograde flow and refute the notion that MII is a motor for retrograde flow. As MII is also implicated in the extension of leading lamellae of migrating cells (Svitkina et al., 1997), it is possible that the coordinate and opposing actions of MIIB and M1c play a similar role in motile cell types such as fibroblasts, macrophages, and invasive cancer cells.

Previous studies have suggested a variety of functional roles for MII. Based on MII localization at sites of lamellipodial retraction in the growth cone, Rochlin et al. (1995) suggested that MII plays a role in retraction. Our findings refute this as we saw retraction when MII was inactivated, suggesting that MII, and specifically MIIB, is required for expansion of lamellipodia. Wylie and Chantler (2001) ascribed a role for neurite extension of MIIB in neuroblastoma cells, since antisense RNA depletion of MIIB inhibited neurite outgrowth. In their studies, neurite length and not extension rate was measured, and growth cone area was not determined. Our results implicate MIIB function in lamellipodial expansion in growth cones, but we observed no instantaneous change in neurite extension rates. Thus, we suggest that chronic application of antisense RNA against MIIB decreased neurite length through prolonged inhibition of lamellipodial expansion. *Xenopus* retinal ganglion cells inhibited with ML-7 showed reduced neurite outgrowth and growth cone collapse, both in vitro and in vivo (Ruchhoeft and Harris, 1997), similar to our pharmacological treatment of chick DRG neurons. Neurons from MIIB-null mutants have shorter neurite lengths after 9–10 h in culture (Tullio et al., 2001) and possessed smaller growth cones with an increased number of protrusions and retractions per minute (Bridgman et al., 2001), although no distinction was made between lamellipodia and filopodia. We observed that inactivation of MII/IIB resulted in reduced growth cone area, and this agrees with results seen with MIIB-null mutant growth cones (Bridgman et al., 2001). We extend this by showing that the reduced area resulted from reduced local lamellipodial protrusion and a reduced net rate of advance of the leading edge, both of which occurred without changes in filopodial extension or retraction. Previously, a small reduction (30%) in filopodial traction force was reported for neurons from MIIB deletion mutants (Bridgman et al., 2001), and it was suggested that MIIA may be responsible for the remaining filopodial traction. However, an MIIA mutant was not tested. Our present findings do not support a role for MIIA and MIIB in filopodial activity. Bridgman et al. (2001) had also observed that the MIIB mutant growth cones had fewer actin bundles. To compare with their result, we examined ALEXA–phalloidin–stained growth cones of DRG neurons and found no obvious differences in F-actin staining profiles in lamellipodia of control (IgG-loaded) and MG-MII-loaded growth cones (unpublished data). The reason for this may be the low numbers of distinct actin bundles in relatively small DRG growth cones.

Micro-CALI of MII resulted in reduced lamellipodial protrusion, and this was associated with a concomitant reduction in diffusive bead movement. However, the precise mechanism of MII action in protrusion and diffusive bead movement remains to be established. We observed lateral bead movements that may underlie the diffusive component of bead motion. These lateral movements may arise from transitions in the bead from one actin filament or bundle to another. Alternatively, the lateral movements may arise from rapid changes in the position of the underlying actin filaments. We favor the possibility that beads make lateral transitions, which may result from the momentary loss of bead coupling to retrograde F-actin flow. Thus, if MII inactivation disrupts cross-linking of the network, a bead proceeding along an actin bundle may have less opportunity to traverse to an adjacent bundle. Further to this idea, a previous study showed that depolymerization of F-actin with cytochalasin B inhibited lateral movement of flow-coupled beads on growth cones (Forscher et al., 1992). Cross-linking between MII filaments and actin bundles in an organized network has been implicated in the protrusion of lamellae in fibroblasts (Verkhovsky et al., 1995). Thus, we suggest that acute inactivation of MII through CALI disrupts actomyosin binding, which leads to a concomitant reduction in MII-medicated cross-linking of actin filaments. A reduction in the cross-linking of F-actin could then impair lamellipodial protrusion, leading to net retraction of the leading edge. Furthermore, our findings refute a role for MII in driving retrograde flow because the loss of such a motor should result in lamellipodial expansion (Lin et al., 1996). Possible effects of MII inactivation include altered ATPase activity, filament formation, or actin binding. The MII antibody recognizes the entire myosin heavy chain, whereas the MIIB antibody is directed to an NH_2-terminal polypeptide sequence in the tail. Since the effects of the two antibodies were similar, it is possible that myosin filament formation was preferentially effected. An NADH-based ATPase assay using HMM showed no effect of the MII or MIIB antibodies on ATPase activity, either in the presence or absence of actin (unpublished data). Unfortunately, a limited supply of antibodies precluded in vitro motility assays to assess how CALI of MII and MIIB affects their function.

Our previous results demonstrated a role for M1c in the retention of lamellipodia (Wang et al., 1996), and our current findings now implicate M1c in retrograde flow. These data support the clutch hypothesis of Mitchison and Kirschner (1988) and ascribe a specific myosin isoform, M1c, in linking retrograde flow to lamellipodial motility (Jay, 2000). In the absence of M1c activity, actin filaments do not proceed retrogradely and β-actin polymerization at the leading edge would then drive protrusion (Fig. 7) (Bassell et al., 1998; Mallavarapu and Mitchison, 1999). How might the action of M1c be linked to retrograde flow? There are two possible roles: it may be a clutch component, or it may be a motor driving actin filaments rearward. We favor its role as a motor driving retrograde flow based on several studies implicating MI in membrane-based cellular activities. MI can associate with the plasma membrane by binding phospholipids through its tail (for review see Coluccio, 1997). Amoeboid MI isoforms are associated with membrane-rich structures such as phagocytic cups and contractile vacuoles and are found in the actin-rich cortex of pseudopodia. Inhibitory antibodies to myoC in *Acanthamoeba* impairs fluid expulsion by contractile vacuoles (Doberstein et al., 1993).

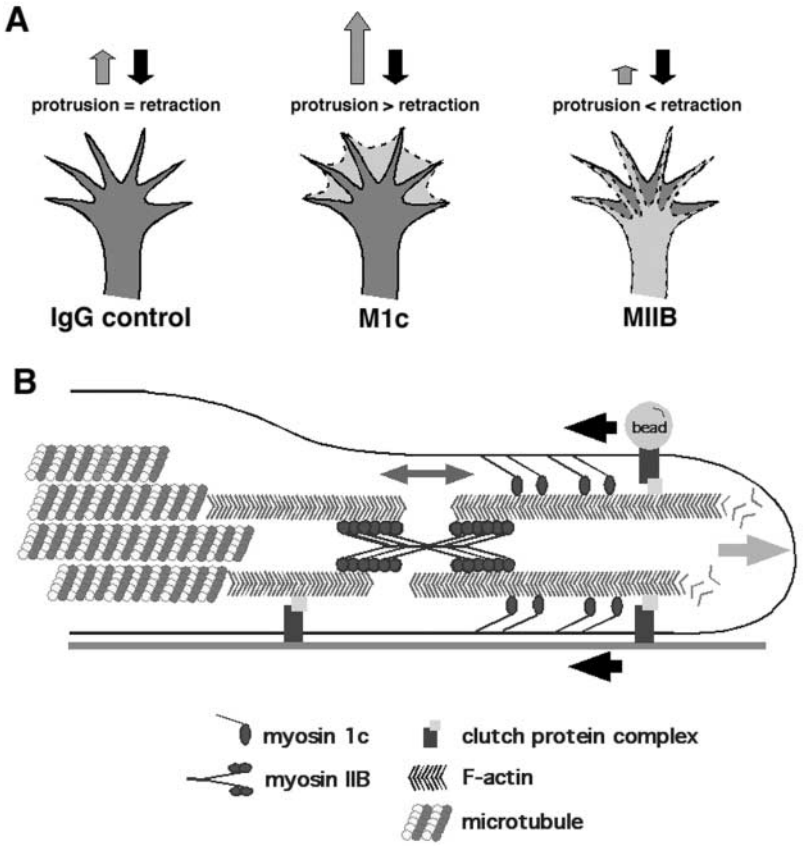

Figure 7. **Suggested roles for M1c and MIIB in lamellipodial dynamics.** (A) Summary of the effects of myosin inactivation on lamellipodial movements. In control IgG-loaded growth cones, local lamellipodial protrusion (gray arrow) and retraction (black arrow) are balanced. When M1c activity is reduced, there is an increase in local lamellipodial protrusion (expanded gray region), and no change in lamellipodial retraction. Conversely, a reduction in MII (or MIIB) activity decreases lamellipodial protrusion (small gray arrow), again without affecting retraction. (B) In a cross section of a leading lamellipodium, M1c may drive F-actin retrogradely (gray arrows) relative to the substrate. When actin filaments are coupled to the substrate through a molecular clutch, retrograde flow slows or stops and leading edge protrusion (large gray arrow) occurs by actin polymerization. MII or the MIIB isoform may cross-link actin filaments. With coupling of F-actin to the substrate, this cross-linking may generate tension across the growth cone (double headed arrow). A reduction in MIIB activity would cause a loss of tension, leading to a reduction in lamellipodial protrusion and net retraction of the leading edge.

Double mutants of myoA/myoB or myoC/myoD in *Dictyostelium* impair fluid uptake via pinocytosis (Novak et al., 1995). MyoB/myoC double mutants show reduced phagocytosis and myoB, C, or D mutations contribute alone or synergistically to endocytosis (Jung et al., 1996). MyoA or myoB mutations result in increased lateral pseudopod formation accompanied by reduced cell locomotion (Titus et al., 1993; Wessels et al., 1991, 1996). Analogous to the reported increases in pseudopod formation, we observed increased lamellipodial protrusion with CALI of M1c in neuronal growth cones. This finding, along with previous mutational analyses in amoebae, suggest that M1c may function in association with growth cone membranes. Furthermore, recent evidence suggests that Myo1c functions as part of an "adaptation motor complex" in hair cells of the inner ear, linking changes in tension through a transduction channel in the membrane to actin filaments of the stereociliary core in a calcium-dependent fashion (Holt et al., 2002). Therefore, it is possible that M1c functions in growth cones to "adapt" to tensile forces in the membrane generated through adhesion and the action of other myosins (discussion of Fig. 7 below). Although the ATPase kinetics of M1c are slow (Zhu et al., 1996), the F-actin translocation rate of M1c is comparable to that of MV, and more than 10-fold greater than brush border MI (Zhu et al., 1996). Indeed, based on the Gillespie model (Holt et al., 2002), the weak binding states of the M1c ATPase cycle might cause M1c to proceed down actin filaments in response to an increase in local tension. Based on these studies and our present findings, we suggest that M1c is the motor which drives retrograde movement of F-actin.

The opposing actions of MIIB and M1c (summarized in Fig. 7 A) suggest a balance of forces across the growth cone mediated by these myosins. This notion is supported by the observation that lamellipodial retraction was greater during asymmetric inactivation of MII than during loss of MII evenly across the whole growth cone. This tension could serve to draw components of the central region forward, if peripheral actin is stably held through coupling to the substrate. Conversely, when adhesion at the leading edge is weak, MIIB-mediated tension may act in growth cone collapse. In contrast to the action of MIIB, we propose that the driving of retrograde F-actin flow by M1c works in conjunction with actin treadmilling. This action moves the actin network rearward to balance the protrusive effect of actin polymerization at the leading edge (Fig. 7 B). When M1c activity is reduced, the leading edge advances through actin polymerization. Local activation of M1c combined with substrate coupling may generate tension. A prediction of this "dynamic tension model" is that an asymmetric change in M1c or MII activity should lead to growth cone turning. Thus, asymmetric changes in MIIB or M1c activity, in conjunction with changes in coupling of F-actin to the substrate, may contribute to growth cone steering or branching.

In view of the opposing actions of M1c and MII on lamellipodial protrusion reported here, it is interesting to note that intracellular calcium can act oppositely on these two myosins. Calcium is a known regulator of growth cone behavior (for review see Kater and Mills, 1991; Zheng et al., 1996). Kater and coworkers postulate that there is a "set-point" of intracellular calcium concentration that is ideal for growth cone motility and that changes in calcium levels can regulate this motility

(Mattson and Kater, 1987). Calcium/calmodulin function is required for appropriate growth cone guidance in *Drosophila* (VanBerkum and Goodman, 1995) and laminin-stimulated turning of chick DRG growth cones (Kuhn et al., 1998). For myosin 1, calmodulin acts as a light chain, which upon binding of calcium, inhibits MI motor activity (Zhu et al., 1998). Conversely, calcium/calmodulin activates MII by increasing myosin light chain kinase activity (Bresnick, 1999). Thus, calcium/calmodulin-dependent pathways may regulate opposing actions of M1c and MII on lamellipodia. One may speculate that local increases in tension may increase calcium at the growth cone leading edge via stretch-sensitive calcium channels as seen in hair cells (Holt et al., 2002). This in turn may cause slippage of M1c along actin filaments (Holt et al., 2002). Indeed, a recent development in the substrate-cytoskeletal coupling model (Suter and Forscher, 2000) suggests that clutch slippage occurs before leading edge advance. Thus, the local balance of M1c and MIIB modulated by calcium signaling may direct growth cone motility and hence act as a downstream effector of axon guidance.

Materials and methods

Neuronal cultures

Chick dorsal root ganglion (DRG) neurons were obtained from stage E9–E11 chick embryos using the method of Sydor et al. (1996). The ganglia were suspended in Ca^{2+}/Mg^{2+}-free HBSS (GIBCO BRL) with 0.25% trypsin/EDTA for 15 min, washed with Ca^{2+}/Mg^{2+}-free HBSS at 37°C, and then dissociated by trituration through a fire-polished glass pipette. The cells were triturated in a combination of MG-labeled antibody solution (1 mg/ml, 40 μl) and 0.2 mg/ml FITC-IgG (Molecular Probes), the latter serving as a fluorescent marker for cell loading. The cells were then spun down at 2,000 rpm (223 *g*) for 30 s, and the pellet was resuspended in culture medium (L-15; Sigma-Aldrich) supplemented with 10% FBS (Hyclone), 25 ng/ml nerve growth factor (7S; Boehringer), gentamycin (Sigma-Aldrich), 0.6% sucrose (Sigma-Aldrich), and 2 mM glutamine (Sigma-Aldrich). The cells were plated in 3 ml of medium on glass-bottomed 35 mm Petri dishes coated with 1 mg/ml poly-L-lysine and 0.1 mg/ml laminin and incubated for 3–6 h at 37°C before observation.

Antibodies and antibody labeling

The rabbit anti-MII polyclonal IgG was raised against intact, native human platelet myosin. In binding assays, it reacted strongly with myosin heavy chain with slight reactivity to myosin light chain and no cross-reactivity with skeletal or smooth muscle myosin (unpublished data; Herman et al., 1981). This antibody showed uniform staining by immunocytochemistry throughout growth cones in a punctate pattern with occasional concentration in filopodia, similar to that observed previously (Miller et al., 1992). A polyclonal anti-MIIB antiserum was raised against the polypeptide sequence SSRSGRRQLHI near the COOH terminus of the chicken MIIB heavy chain (a gift from Dr. Robert Adelstein, National Heart, Lung, and Blood Institute, National Institutes of Health, Bethesda, MD) (Kelley et al., 1996). The polyclonal MIIA antibody against human platelet myosin (Kelley and Adelstein, 1990) was obtained commercially (Biomedical Technologies, Inc.). Western blots with stage E10 chick DRG lysates showed affinity to MII heavy chains, and isoform antibodies showed affinity for A and B heavy chains as reported previously (Kelley et al., 1996). A monoclonal antibody against M1c (previously myosin Iβ [Wagner et al.,1992] from clone M2 which recognizes the tail domain) was a gift from Mark Wagner (Indiana University Medical Center, Indianapolis, IN) and was previously used for CALI of M1c (myosin Iβ [Wang et al., 1996]). Labeling of antibodies with MG (MGITC; Molecular Probes) was performed as described previously (Beermann and Jay, 1994). To control for nonspecific effects of antibody loading and laser irradiation, growth cones were loaded with an MG-labeled, nonimmune, rabbit IgG (Pierce Chemical Co.).

Pharmacological experiments

To test the response of chick DRG growth cones to pharmacological inhibition of MII, the specific inhibitor, 1-(5-isoquinoline sulfonyl)-2-methyl piperazine (ML-7) was employed. ML-7 inhibits the myosin light chain kinase through competitive binding of the ATP-binding site (Saitoh et al., 1987). ML-7 was bath applied to cultures for 5 min followed by washout with culture media. The final concentrations tested were 1.0, 5.0, and 10 μM for ML-7, with 0.01% DMSO vehicle serving as a control. Cultures were imaged before and during the addition of drug using a Nikon Diaphot 200 inverted epifluorescence microscope (40× Plan Apo, 0.95 NA) coupled with a cooled CCD camera (Orca, Hamamatsu). Commercial imaging software (Openlab, Improvision Inc.) was used to capture and process images. Growth cone area was quantified at 1-min intervals and normalized to the initial pretreatment area. Growth cone collapse was scored when growth cones displayed complete loss of lamellipodia and filopodia and assumed a club-shaped morphology. In every instance of collapse observed, growth cones also lost adhesion and retracted. Unless noted otherwise in the text, statistical comparisons between treatment groups in these and other experiments were performed using Student's two-tailed, unpaired *t* test with 95% confidence limits.

CALI of myosin and neurite outgrowth

Large scale CALI was performed as described previously (Wang et al., 1996). Briefly, cells where plated onto glass coverslips that were marked as two halves: one half received laser irradiation and the other half served as a matched control. Neurons loaded with antibodies against MII, MIIB, or MIIA were irradiated for 2 min and then permitted to extend neurites for 1 h. At the end of the 1-h period, the cells were fixed with ice-cold 4% paraformaldehyde in PBS with 30% sucrose for 15 min, washed in PBS, and then imaged. Changes in neurite length and growth cone area were quantified using commercial software (Openlab, Improvision Inc.).

Micro-CALI of M1c and MII

Neurons were loaded with either MG-labeled myosin antibody or a nonspecific MG-IgG antiserum as described above. Cultures were observed using a Nikon Diaphot 200 inverted microscope with a stage incubator set at 37°C (Opti-Quip, Inc.). Growth cones were observed for 10 min before micro-CALI. Images were captured as described above at 15-s intervals using a cooled CCD camera and imaging software. Growth cones were irradiated either in their entirety or on one half with the unirradiated half serving as an internal control. Growth cone halves were defined by an axis orthogonal to and bisecting 20 μm of neurite proximal to the growth cone. Growth cones were irradiated for 5 min in all experiments using a nitrogen-pumped dye laser (model VSL-337ND; Laser Science, Inc.). The laser wavelength was 620 nm, pulse width was 3.5 ns, and pulse frequency was 30 Hz, with an average single pulse energy of 30 μJ. The laser spot size was ~10 μm in diameter. Growth cones were imaged using phase–contrast optics (40× Plan Apo, 0.95 NA; Nikon) during laser irradiation and for up to 30 min after irradiation. The rate of forward advance of the growth cone was determined by measuring movement of the neurite neck (Li et al., 1994). The rate of lamellipodial extension was determined by measuring changes in the rate of the leading edge of the lamellipodium at the central axis of the growth cone (the axis parallel to the proximal 20 μm of neurite and bisecting the neurite neck). Since total growth cone area was quantified rather than lamellipodial area, any difference in area observed is normalized to the total growth cone area rather than the area of lamellipodia. Since the central growth cone region likely contributes little to changes in area resulting from changes in lamellipodial activity, any change in growth cone area underestimates any effect on lamellipodia alone.

Microbead assays

Retrograde F-actin flow was assayed using a microbead-binding method developed previously (Forscher et al., 1992; Lin and Forscher, 1995). Polystyrene microbeads (200 nm diameter) were washed in L-15 culture medium, spun down, and resuspended at 1:1000 dilution in 200 μl culture medium. Only beads that adhered to the lamellipodial region of growth cones and remained attached for at least 9 s (three consecutive image capture intervals) were selected for observation. Since the beads were uncoated and have a net negative charge, sustained attachment of beads would likely be mediated by electrostatic, nonspecific interactions with plasma membrane constituents. Upon stable attachment of a bead, images were captured at 3-s intervals using the imaging apparatus described. Growth cones with beads proceeding centripetally were then irradiated for ~5 min. Imaging was halted if beads contacted the clearly delineated transition zone (margin of the peripheral lamellipodial region and the central region), since it is known that retrograde flow of actin ceases in the transition zone. Observations of bead movements were confined to lamellipodia because of the difficulty observing bead movement on DRG growth cone filopodia, which occasionally lose contact with the substratum and display "waving" movements.

Two parameters of bead movement were quantified: rate of directed, nonrandom motion and rate of diffusive, random motion. These parameters were determined by mean squared displacement analysis of point-by-point transitions of individual beads on a two-dimensional coordinate plane. From individual x,y coordinates the mean squared displacement (MSD) was calculated for each time interval using custom Unix-based software (written by Dr. Canwen Liu). Using the equation $<d^2> = (vt)^2 + 4Dt$, a regression analysis of MSD values for different time intervals was performed. By fitting the data with the equation using Origin software (Originlabs), coefficients were obtained which indicate the degree of directed motion and random motion of the bead movement (Schmidt et al., 1993, 1995). The coefficients of directed and diffusive movement were then averaged for the different treatments.

This work is dedicated to the memory of Mr. Bernard (Bernie) Ludwig Diefenbach.

The authors thank Dr. Andrea Buchstaller, Ms. Brenda Eustace, and Ms. Jean Stewart for helpful comments on the manuscript, and Dr. Buchstaller for valuable discussion. We also thank Mr. Craig Thalhauser for helpful discussions and assistance with the MSD program.

This work supported by the National Institutes of Health grants (NS34699 and EY11992 to D.G. Jay; GM55110, EY90933, and DKSP3034928 to I.M. Herman). V.M. Latham was supported in part by a training grant (DK07542).

Submitted: 7 February 2002
Revised: 16 August 2002
Accepted: 20 August 2002

References

Bahler, M., R. Kroschewski, H.E. Stoffler, and T. Behrmann. 1994. Rat myr 4 defines a novel subclass of myosin I: identification, distribution, localization, and mapping of calmodulin-binding sites with differential calcium sensitivity. *J. Cell Biol.* 126:375–389.

Bassell, G.J., H. Zhang, A.L. Byrd, A.M. Femino, R.H. Singer, K.L. Taneja, L.M. Lifshitz, I.M. Herman, and K.S. Kosik. 1998. Sorting of β-actin mRNA and protein to neurites and growth cones in culture. *J. Neurosci.* 18:251–265.

Beermann, A.E., and D.G. Jay. 1994. Chromophore-assisted laser inactivation of cellular proteins. *Methods Cell Biol.* 44:715–732.

Berg, J.S., B.C. Powell, and R.E. Cheney. 2001. A millenial myosin census. *Mol. Biol. Cell.* 12:780–794.

Bresnick, A.R. 1999. Molecular mechanisms of nonmuscle myosin-II regulation. *Curr. Opin. Cell Biol.* 11:26–33.

Bridgman, P.C., S. Dave, C.F. Asnes, A.N. Tullio., and R.S. Adelstein. 2001. Myosin IIB is required for growth cone motility. *J. Neurosci.* 21:6159–6169.

Buchstaller, A., and D.G. Jay. 2000. Micro-scale chromophore-assisted laser inactivation of nerve growth cone proteins. *Microsc. Res. Tech.* 48:97–106.

Cheng, T.P., N. Murakami, and M. Elzinga. 1992. Localization of myosin IIB at the leading edge of growth cones from rat dorsal root ganglionic cells. *FEBS Lett.* 311:91–94.

Cheung, A., J.A. Dantzig, S. Hollingworth, S.M. Baylor, Y.E. Goldman, T.J. Mitchison, and A.F. Straight. 2002. A small-molecule inhibitor of skeletal muscle myosin II. *Nat. Cell Biol.* 4:83–88.

Coluccio, L.M. 1997. Myosin I. *Am. J. Physiol.* 273:C347–C359.

Danuser, G., and R. Oldenbourg. 2000. Probing F-actin flow by tracking shape fluctuations of radial bundles in lamellipodia of motile cells. *Biophys. J.* 79: 191–201.

Dent, E.W., and K. Kalil. 2001. Axon branching requires interactions between dynamic microtubules and actin filaments. *J. Neurosci.* 21:9757–9769.

Doberstein, S.K., I.C. Baines, G. Wiegand, E.D. Korn, and T.D. Pollard. 1993. Inhibition of contractile vacuole function *in vivo* by antibodies against myosin-I. *Nature.* 365:841–843.

Forscher, P., and S.J. Smith. 1988. Actions of cytochalasins on the organization of actin filaments and microtubules in a neuronal growth cone. *J. Cell Biol.* 107:1505–1516.

Forscher, P., C.H. Lin, and C. Thompson. 1992. Novel form of growth cone motility involving site-directed actin filament assembly. *Nature.* 357:515–518.

Gillespie, P.G., J.P. Albanesi, M. Bahler, W.M. Bement, J.S. Berg, D.R. Burgess, B. Burnside, R.E. Cheney, D.P. Corey, E. Coudrier, et al. 2001. Myosin-I nomenclature. *J. Cell Biol.* 155:703–704.

Hasson, T., and M.S. Mooseker. 1997. The growing family of myosin motors and their role in neurons and sensory cells. *Curr. Opin. Neurobiol.* 7:615–623.

Herman, I.M., N.J. Crisona, and T.D. Pollard. 1981. Relation between cell activity and the distribution of cytoplasmic actin and myosin. *J. Cell Biol.* 90:84–91.

Holt, J.R., S.K.H. Gillespie, D.W. Provance, Jr., K. Shah, K.M. Shokat, D.P. Corey, J.A. Mercer, and P.G. Gillespie. 2002. A chemical-genetic strategy implicates myosin-1c in adaptation by hair cells. *Cell.* 108:371–381.

Jay, D.G. 1988. Selective destruction of protein function by chromophore-assisted laser inactivation. *Proc. Natl. Acad. Sci. USA.* 85:5454–5458.

Jay, D.G. 2000. The clutch hypothesis revisited: ascribing the roles of actin-associated proteins in filopodial protrusion in the nerve growth cone. *J. Neurobiol.* 44:114–125.

Jung, G., X. Wu, and J.A. Hammer, III. 1996. *Dictyostelium* mutants lacking multiple classic myosin I isoforms reveal combinations of shared and distinct functions. *J. Cell Biol.* 133:305–323.

Kater, S.B., and L.R. Mills. 1991. Regulation of growth cone behavior by calcium. *J. Neurosci.* 11:891–900.

Kelley, C.A., and R.S. Adelstein. 1990. The 204-kDa smooth muscle myosin heavy chain is phosphorylated in intact cells by casein kinase II on a serine near the carboxyl terminus. *J. Biol. Chem.* 265:17876–17882.

Kelley, C.A., J.R. Sellers, D.L. Gard, D. Bui, R.S. Adelstein, and I.C. Baines. 1996. *Xenopus* nonmuscle myosin heavy chain isoforms have different subcellular localizations and enzymatic activities. *J. Cell Biol.* 134:675–687.

Kuhn, T.B., C.V. Williams, P. Dou, and S.B. Kater. 1998. Laminin directs growth cone navigation via two temporally and functionally distinct calcium signals. *J. Neurosci.* 18:184–194.

Li, G.H., C.D. Qin, and M.H. Li. 1994. On the mechanism of growth cone locomotion: modeling and computer simulation. *J. Theor. Biol.* 169:355–362.

Lin, C.H., and P. Forscher. 1995. Growth cone advance is inversely proportional to retrograde F-actin flow. *Neuron.* 14:763–771.

Lin, C.H., E.M. Espreafico, M.S. Mooseker, and P. Forscher. 1996. Myosin drives retrograde F-actin flow in neuronal growth cones. *Neuron.* 16:769–782.

Lu, M., W. Witke, D.J. Kwiatkowski, and K.S. Kosik. 1997. Delayed retraction of filopodia in gelsolin null mice. *J. Cell Biol.* 138:1279–1287.

Mallavarapu, A., and T. Mitchison. 1999. Regulated actin cytoskeleton assembly at filopodium tips controls their extension and retraction. *J. Cell Biol.* 146: 1097–1106.

Mattson, M.P., and S.B. Kater. 1987. Calcium regulation of neurite elongation and growth cone motility. *J. Neurosci.* 7:4034–4043.

Miller, M., E. Bower, P. Levitt, D. Li, and P.D. Chantler. 1992. Myosin II distribution in neurons is consistent with a role in growth cone motility but not synaptic vesicle mobilization. *Neuron.* 8:25–44.

Mitchison, T., and M. Kirschner. 1988. Cytoskeletal dynamics and nerve growth. *Neuron.* 1:761–772.

Novak, K.D., M.D. Peterson, M.C. Reedy, and M.A. Titus. 1995. *Dictyostelium* myosin I double mutants exhibit conditional defects in pinocytosis. *J. Cell Biol.* 131:1205–1221.

Rochlin, M.W., K. Itoh, R.S. Adelstein, and P.C. Bridgman. 1995. Localization of myosin II A and B isoforms in cultured neurons. *J. Cell Sci.* 108:3661–3670.

Ruchhoeft, M.L., and W.A. Harris. 1997. Myosin functions in *Xenopus* retinal ganglion cell growth cone motility *in vivo*. *J. Neurobiol.* 32:567–578.

Ruppert, C., R. Kroschewski, and M. Bahler. 1993. Identification, characterization and cloning of myr 1, a mammalian myosin-I. *J. Cell Biol.* 120:1393–1403.

Saitoh, M., T. Ishikawa, S. Matsushima, M. Naka, and H. Hidaka. 1987. Selective inhibition of catalytic activity of smooth muscle myosin light chain kinase. *J. Biol. Chem.* 262:7796–7801.

Schmidt, C.E., A.F. Horwitz, D.A. Lauffenburger, and M.P. Sheetz. 1993. Integrin-cytoskeletal interactions in migrating fibroblasts are dynamic, asymmetric and regulated. *J. Cell Biol.* 123:977–991.

Schmidt, C.E., J. Dai, D.A. Lauffenburger, M.P. Sheetz, and A.F. Horwitz. 1995. Integrin-cytoskeletal interactions in neuronal growth cones. *J. Neurosci.* 15: 3400–3407.

Suter, D.M., and P. Forscher. 2000. Substrate-cytoskeletal coupling as a mechanism for the regulation of growth cone motility and guidance. *J. Neurobiol.* 44:97–113.

Suter, D.M., F.S. Espindola, C.H. Lin, P. Forscher, and M.S. Mooseker. 2000. Localization of unconventional myosins V and VI in neuronal growth cones. *J. Neurobiol.* 42:370–382.

Svitkina, T.M., A.B. Verkhovsky, K.M. McQuade, and G.G. Borisy. 1997. Analysis of the actin-myosin II system in fish epidermal keratocytes: mechanism of cell body translocation. *J. Cell Biol.* 139:397–415.

Sydor, A.M., A.L. Su, F.S. Wang, A. Xu, and D.G. Jay. 1996. Talin and vinculin play distinct roles in filopodial motility in the neuronal growth cone. *J. Cell*

Biol. 134:1197–1207.

Titus, M.A., D. Wessels, J.A. Spudich, and D. Soll. 1993. The unconventional myosin encoded by the myoA gene plays a role in Dictyostelium motility. *Mol. Biol. Cell.* 4:233–246.

Tullio, A.N., P.C. Bridgman, N.J. Tresser, C.C. Chan, M.A. Conti, R.S. Adelstein, and Y. Hara. 2001. Structural abnormalities develop in the brain after ablation of the gene encoding nonmuscle myosin II-B heavy chain. *J. Comp. Neurol.* 433:62–74.

VanBerkum, M.F., and C.S. Goodman. 1995. Targeted disruption of Ca(2+)-calmodulin signaling in *Drosophila* growth cones leads to stalls in axon extension and errors in axon guidance. *Neuron.* 14:43–56.

Verkhovsky, A.B., T.M. Svitkina, and G.G. Borisy. 1995. Myosin II filament assemblies in the active lamella of fibroblasts: their morphogenesis and role in the formation of actin filament bundles. *J. Cell Biol.* 131:989–1002.

Wagner, M.C., B. Barylko, and J.P. Albanesi. 1992. Tissue distribution and subcellular localization of mammalian myosin I. *J. Cell Biol.* 119:163–170.

Wang, F.S., J.S. Wolenski, R.E. Cheney, M.S. Mooseker, and D.G. Jay. 1996. Function of myosin-V in filopodial extension of neuronal growth cones. *Science.* 273:660–663.

Wessels, D., J. Murray, G. Jung, J.A. Hammer, III, and D.R. Soll. 1991. Myosin IB null mutants of Dictyostelium exhibit abnormalities in motility. *Cell Motil. Cytoskeleton* 20:301–315.

Wessels, D., M. Titus, and D.R. Soll. 1996. A Dictyostelium myosin I plays a crucial role in regulating the frequency of pseudopods formed on the substratum. *Cell Motil Cytoskel.* 33:64–79.

Welnhofer, E.A., L. Zhao, and C.S. Cohan. 1999. Calcium influx alters actin bundle dynamics and retrograde flow in Helisoma growth cones. *J. Neurosci.* 19: 7971–7982.

Wylie, S.R., and P.D. Chantler. 2001. Separate but linked functions of conventional myosins modulate adhesion and neurite outgrowth. *Nat. Cell Biol.* 3:88–92.

Wylie, S.R., P.J. Wu, H. Patel, and P.D. Chantler. 1998. A conventional myosin motor drives neurite outgrowth. *Proc. Natl. Acad. Sci. USA.* 95:12967–12972.

Zheng, J.Q., M.-M. Poo, and J.A. Connor. 1996. Calcium and chemotropic turning of nerve growth cones. *Perspect. Dev. Neurobiol.* 4:205–213.

Zhu, T., K. Beckingham, and M. Ikebe. 1998. High affinity Ca^{2+} binding sites of calmodulin are critical for the regulation of myosin Iβ motor function. *J. Biol. Chem.* 273:20481–20486.

Zhu, T., M. Sata, and M. Ikebe. 1996. Functional expression of mammalian myosin I beta: analysis of its motor activity. *Biochemistry.* 35:513–522.